

## Article

# Study on the Strength and Microcosmic Characteristics of C50 High-Performance Concrete (HPC) Containing Manufactured Sands

Yafeng Hu , Yang Wei , Longlong Zhao, Wenhua Zhang and Si Chen

School of Civil Engineering, Nanjing Forestry University, Nanjing 210037, China

\* Correspondence: wy78@njfu.edu.cn

**Abstract:** In this paper, C50 high-performance concrete (HPC) containing manufactured sand was prepared. First, three different gradations of aggregates and three different types of admixtures with significant differences in specific surface area, porosity, and water ratios were used to prepare nine groups of concrete mixtures. Second, the effect of the aggregate gradation and admixture on the workability of fresh HPC and compressive strength of hydration-hardened HPC was investigated. Finally, microscopic tests were conducted to examine the hydration product pore structure (mercury injection porosimeter (MIP)), hydration product surface appearance (scanning electron microscope (SEM)), and element qualitative analysis (energy dispersive X-ray spectrometry (EDS)), and the mechanism of the C50 HPC was discussed. The results show that the types of gradation aggregates and admixtures significantly affect the workability and strength of C50 HPC. When the slump of fresh HPC is specified, the workability of the mixture can be controlled by a homemade high-performance lignin sulfonate water reducer. The aggregate gradation biased toward the median of the gradation curve can be used to prepare the C50 HPC. In this paper, the maximum compressive strength of C50 HPC is 58.3 MPa at 90 days. In addition, the microscopic test results show that the composite compound of C50 HPC has a dense hydration product and a high bond strength interface transition zone (ITZ).

**Keywords:** HPC; manufactured sand; strength characteristics; MIP; ITZ



**Citation:** Hu, Y.; Wei, Y.; Zhao, L.; Zhang, W.; Chen, S. Study on the Strength and Microcosmic Characteristics of C50 High-Performance Concrete (HPC) Containing Manufactured Sands. *Buildings* **2022**, *12*, 1657. <https://doi.org/10.3390/buildings12101657>

Academic Editor: Arslan Akbar

Received: 14 September 2022

Accepted: 8 October 2022

Published: 11 October 2022

**Publisher's Note:** MDPI stays neutral with regard to jurisdictional claims in published maps and institutional affiliations.



**Copyright:** © 2022 by the authors. Licensee MDPI, Basel, Switzerland. This article is an open access article distributed under the terms and conditions of the Creative Commons Attribution (CC BY) license (<https://creativecommons.org/licenses/by/4.0/>).

## 1. Introduction

Since the beginning of the 21st century, the civil engineering field of China has rapidly developed, the annual amount of concrete used ranks among the top in the world, and natural resources, including mines and rivers, have been seriously damaged due to the demands of project construction [1,2]. In recent years, with the implementation of environmental protection policies and the increase in people's environmental awareness, the utilization of industrial scrap and waste mineral materials [3,4] in projects has increased. Tunnel and road excavation projects can produce a large quantity of aggregate rocks and, if they are not scientifically used, they require higher transportation costs and pollute the environment by piling up and littering. Manufactured sand [5,6], which is crushed and selected in the aggregate rock, can partially or completely replace the natural aggregate and be applied in concrete projects [7–10]. As shown in Figure 1, Manufactured sand has an angular and small specific surface area and a large porosity among the particles. Therefore, the use of manufactured sand as a concrete aggregate will lead to the disadvantageous workability of fresh concrete, including mobility and cohesiveness.



**Figure 1.** Manufactured sand. (a) Excavated tunnel; (b) Manufactured sand.

There are several advantages of using superfine powders, such as fly ash (FA) [11,12], silica fume (SF) [13–15], and red mud powder (RM) [16] as the admixtures to fill the manufactured sand gap. First, the mobility of fresh concrete will be improved because these micropowder particles are spherical. Second, FA, SF, and RM contain active metal oxides that react with volcanic ash in concrete and cement paste to form new minerals, which enrich the mineral composition of the concrete matrix and enhance the adhesion properties between the matrix and the manufactured sand [17]. Third, the small particle sizes of the admixture form a good filling effect and improve the compactness in concrete [18]. Fourth, these admixtures belong to industrial refuse and mine tailings, and applying them to concrete can increase environmental protection and turn waste into treasure. However, the admixture improves the workability and compactness of manufactured sand concrete [19,20], which actually decreases the proportion of aggregate and increases the proportion of cement and admixture. These changes may have disadvantage effects, including cracks in concrete hydration, exothermic heat, dry shrinkage cracks [21] in the curing stage, and even early deterioration of concrete. Therefore, how to optimize the material composition of HPC, use an efficient thickening water reducer [22,23], adjust the mixing steps of admixtures, and eliminate the negative impact of the angularity of manufactured sand on the segregation and water secretion of fresh concrete are the key problems in the application of HPC in practical engineering.

Our studies have discussed the preparation of C50 HPC using the following methods. First, the crushing value of manufactured sand satisfies the requirements of the current Euro code of EN 12620-2002 [24]. Second, high-quality FA, SF, and RM were substituted for Portland cement material. Finally, the mixing steps of HPC were optimized, and a homemade, efficient lignin sulfonate [25] water reducer was used to regulate the consistency and water reduction rate of fresh concrete. With this method, a green, eco-friendly C50 HPC with a lower production cost was successfully prepared.

In this paper, C50 HPC with manufactured sand and no obvious performance difference compared to traditional concrete was investigated. The mixture was prepared using three different types of grading (coarse mesh size (MS-C), middle mesh size (MS-M) and fine mesh size (MS-F)) and three different types of admixture, which had significant differences in specific surface area, porosity of the mineral, aggregate, and water ratios. The effects of the aggregate gradation and admixture type on the workability of fresh HPC and compressive strength of hardened HPC were investigated [26]. Microscopic tests were conducted, such as mercury injection porosimetry (MIP), scanning electron microscopy (SEM), and energy dispersive X-ray spectrometry (EDS). The mechanism of the C50 HPC was discussed.

## 2. Specimen Design

### 2.1. Materials

One type of binding material was used in this study: Portland cement (PC) with 28 days of compressive strength of 68.9 MPa and 6.7 Mpa; Code: P-II 42.5R (Anhui Conch Cement Co., Ltd., Wuhu, China); three types of admixture: first-grade and low-calcium FA (Nanjing Iron & Steel Co., Ltd., Nanjing, China), SF (Guangzhou Shinshi Metallurgical and Chemical Co., Ltd., Guangzhou, China) and RM (Huanglongshan, Yixing, Jiangsu, China). The chemical compositions and physical properties are shown in Table 1, and the particle size compositions are shown in Figure 2. The efficient water reducer in this experiment is lignin sulfonate.

**Table 1.** Chemical composition and physical properties of the binding materials.

Chemical Composition (%)	PC	FA	SF	RM
SiO <sub>3</sub>	19.8	36.9	93.6	66.3
Fe <sub>2</sub> O <sub>3</sub>	4.2	6.3	1.7	6.2
MgO	4.7	8.6	1.2	0.7
Al <sub>2</sub> O <sub>3</sub>	5.3	11.2	0.2	3.6
CaO	61.7	32.9	1.5	21.6
SO <sub>3</sub>	2.1	1.8	1.1	1.2
LOI	2.2	2.3	0.7	0.4
Specific surface area (m <sup>2</sup> /kg)	396	263	2150	1390
Specific gravity (kg/m <sup>3</sup> )	3.12	2.66	1.87	1.86

Manufactured sand with a maximum size of 37.5 mm was used as the aggregate, as shown in Figure 3, and natural aggregate was not used in this experiment. According to the requirements of the current Euro code of EN 12620-2002, the aggregate gradation is divided into three types: coarse mesh size (MS-C), middle mesh size (MS-M), and fine mesh size (MS-F). The three groups of grading curves approach the lower limit, middle value and upper limit of the specification in EN 12620-2002, as shown in Figure 3.

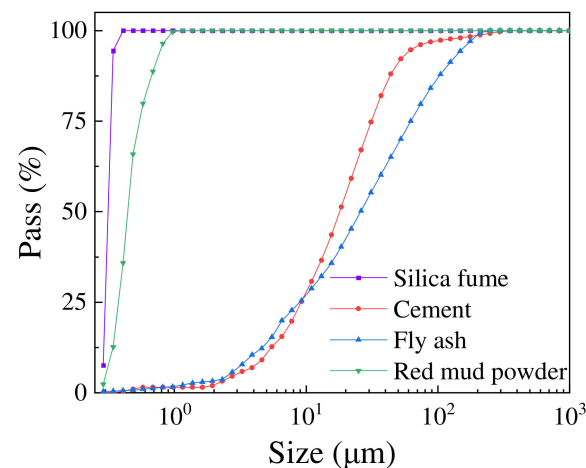


**Figure 2.** Particle size compositions of cement and admixtures.

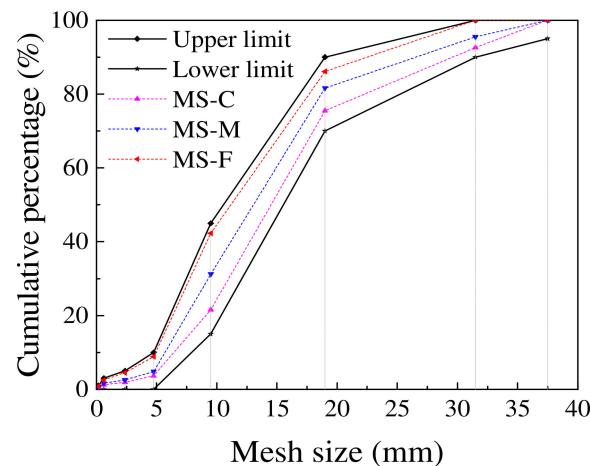


**Figure 3.** Manufactured sand aggregate gradation curve.

## 2.2. Mix-Design

Ten groups of mixtures were designed. One reference concrete (RC) had a middle mesh size (MS-M) without admixture; nine mixtures with aggregates, binding materials and admixtures were designed, and the mixture proportions are shown in Table 2. There are the following regulations on the workability of fresh HPC mixed by each group of mixtures. First, according to the provisions of the Euro code of EN 12350-2-1999 [27], the expansion value of fresh HPC is 700 mm in each group. Second, 15% of cement was replaced by admixtures. Third, when the expansion of fresh HPC is not 700 mm, the mixture should be remixed under the condition of only adjusting the water consumption and water-reducing agent. As specified above, the total material composition of each group HPC obtained by test mixing is shown in Table 2.

**Table 2.** HPC material proportions ( $\text{kg}/\text{m}^3$ ).

Mix No.	Water	Cement	FA	SF	RM	Fine MS Aggregate	Coarse MS Aggregate	Super Plasticizer
RC	193	485	0	0	0	676	862	1.46
MS-C-1	196	410	75	0	0	555	983	1.52
MS-C-2	204	410	60	15	0	555	983	1.52
MS-C-3	212	410	50	10	15	555	983	1.49
MS-M-1	204	410	75	0	0	676	862	1.48
MS-M-2	215	410	60	15	0	676	862	1.49
MS-M-3	228	410	50	10	15	676	862	1.51
MS-F-1	218	410	75	0	0	758	780	1.48
MS-F-2	232	410	60	15	0	758	780	1.49
MS-F-3	246	410	50	10	15	758	780	1.49

## 2.3. Concrete Mixture and Specimen Preparation

First, the cement, admixture and fine aggregate (manufactured sand particle size below 4.75 mm) were dry-mixed for 1 min. Second, the mixture of water and water reducer was added and stirred for 2 min. Third, the coarse aggregate was added to the mortar and mixed for 2 min. Fourth, 10 L of fresh concrete was removed, and the expansion values of fresh concrete were detected. If the expansion value was less than 700 mm, a small amount of water and water reducer was added to the mix until the detected expansion values reached 700 mm. During this period, if the concrete mixture in the mix is poorly adhered, a tiny amount of lignin can be added as appropriate to thicken the concrete mixture.

The fresh C50 HPC was cast into a  $\phi 150 \text{ mm} \times 150 \text{ mm}$  mold, compacted by a vibrating table, put into a standard concrete curing box ( $20 \pm 2 \text{ }^\circ\text{C}$  and 98% relative humidity), dismantled after 24 h, and cured to the specified date.

### 3. Testing Methods of Expansion, Compressive Strength and Microscopic Character

#### 3.1. Fluidity Tests

Fresh HPC mixture properties were determined using the expansion test for workability in accordance with the Euro code of EN 12350-2-1999. The test device consists of a conical slump cylinder and a flat steel plate with dimensions of 1000 mm × 1000 mm and circular expansion engraved on the surface, as shown in Figure 4.

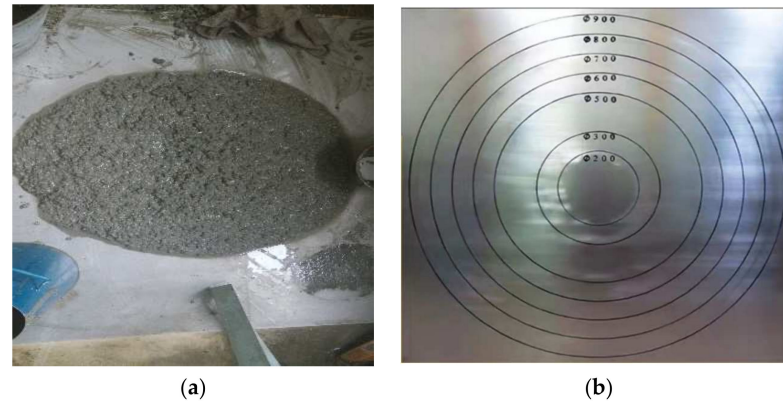


**Figure 4.** Concrete expansion test. (a) Expansion test; (b) The steel plate.

#### 3.2. Compressive Strength Test

A closed-loop servo-controlled material testing machine (Shenzhen SUNS Technology Stock Co., Ltd., Shenzhen, China) was used to conduct the compressive strength test according to the Euro code of EN 12390-3-2001 [28]. The compressive strength test of HPC was performed on  $\phi 150$  mm × 150 mm cylinder specimens, the loading mode was force control, and the loading rate was 1 MPa/s until the cube HPC specimens were destroyed.

The compressive strength of HPC was standard cured for 3, 7, 28, and 90 days in accordance with the Euro code of EN 12390-3-2001 and literatures [29,30]. Three specimens from each group were tested to determine the compressive strength, as shown in Figure 5.



**Figure 5.** Schematic of compressive strength.

#### 3.3. Microscopic Character Test

To study the details of the interfacial transition zone (ITZ) between hardened cement paste and manufactured sand aggregates after the hydration of cement material and admixture, SEM (AXIS Supra photoelectron spectrometer, Shimadzu, Kyoto, Japan) and MIP (AutoPore IV 9510, Micromeritics, Norcross, GA, USA) measurements were performed. To obtain representative samples, the samples analyzed by microcosmic were from the central position of the HPC broken specimens in the compression test. The detected sample

thickness was 1–2 mm, and the sample size was approximately 10 mm × 10 mm. Then, the sample was placed into a brown bottle containing acetone, hydrated and labeled. When used for testing, the sample was removed, placed and dried in vacuum desiccators (temperature 120 °C, pressure −0.1 MPa) to constant weight. The HPC specimen for SEM first required a spray gold treatment and formed a conductive film on the surface.

## 4. Results and Discussion of the Fresh Concrete and Compressive Strength

### 4.1. Fresh Concrete Workability

When the fresh concrete expansion value reached 700 mm, the water demand of each group mixture is shown in Figure 6. It clearly shows that the composite admixture concrete requires more water than the reference group. If the types of mixture and the quantity of mixture are equal, the change trend of water demand with the mechanical aggregate gradation is that finer aggregate has greater water demand. This phenomenon is directly related to the specific surface area of the total mineral particle composition of each group of mixtures.

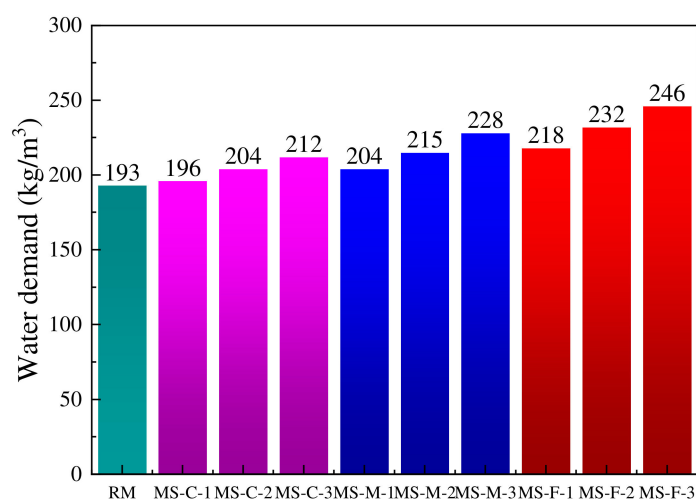


**Figure 6.** Water demand of each concrete group.

### 4.2. Compressive Strength

The compressive strength development of HPC mixtures without and with the admixture of manufactured sand is presented in Figure 7. The data in Figure 7 indicate that the use of an admixture of manufactured sand obviously affects the compressive strength of HPC. As shown in Figure 7, the compressive strength of HPC mixed with FA at 90 days of age was 41.2 MPa, which was higher than 35.5 MPa of the RC group. However, the compressive strength of HPC mixed with the double mixture powder was 52.6 MPa, and that with triple mixtures was 58.5 MPa. Therefore, the mixtures have a good filling effect, participate in the hydration reaction, and exhibit a “superposition effect”. As a result, composite mixtures significantly affect the compressive strength of manufactured sand HPC.

For single mixtures, double mixtures, and triple mixtures, the compressive strength of HPC with variable gradating types at 90 days is shown in Figure 8. The test results indicate that gradating aggregates significantly affect the compressive strength of HPC. For the single mixture (FA) of HPC, the compressive strength gradually decreases with the grading from coarse to fine. However, for the double mixtures (FA and SF) and triple mixtures (FA, SF, and RM) of HPC, the compressive strength first increased and subsequently decreased with the grading from coarse to fine. Figure 5 clearly shows that with a single mixture, double mixtures, and triple mixtures, the maximum compressive strength of fine-graded HPC is 21.8% and 25.1% lower than that of the other two gradating cases, respectively. Thus, the appropriate gradation form of manufactured sand helps improve the compressive strength of HPC, but a fine gradation of aggregate tends to reduce the HPC strength.

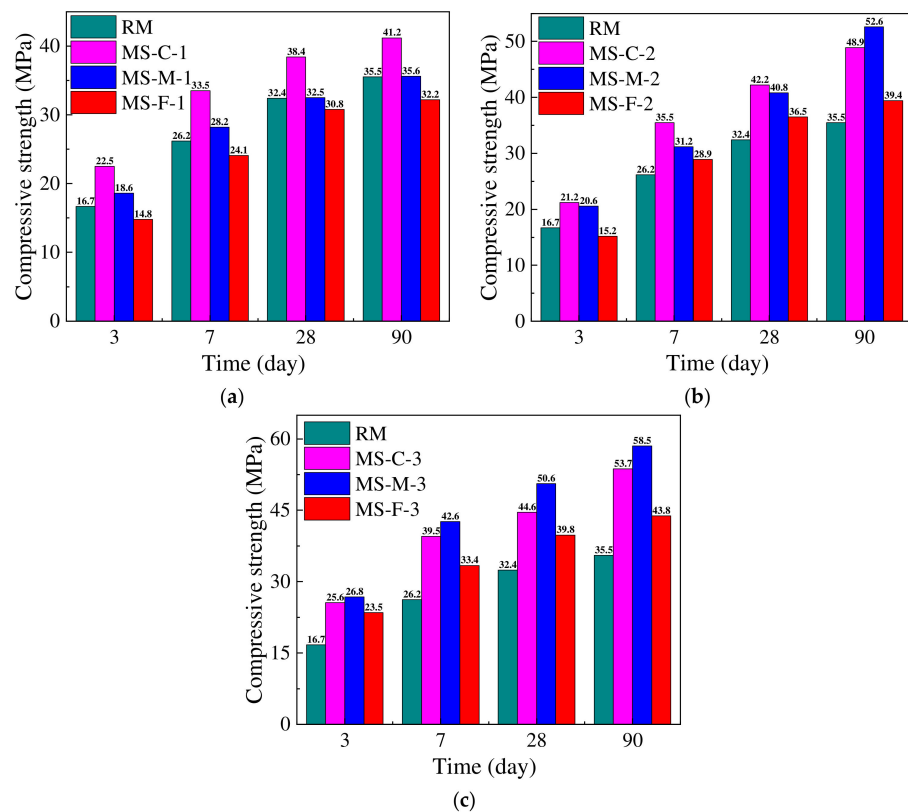


**Figure 7.** Influence of the admixtures on the HPC compressive strength. (a) HPC compressive strength of FA; (b) HPC compressive strength of FA and SF; (c) HPC compressive strength of FA, SF and RM.

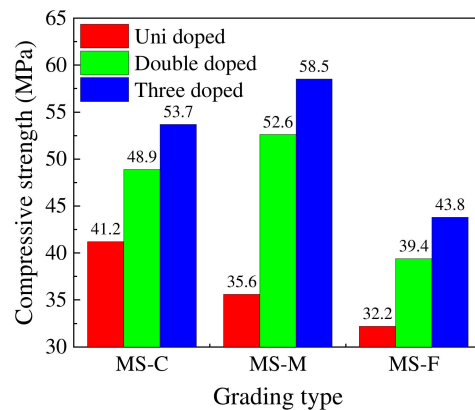


**Figure 8.** Influence of gradation on the HPC compressive strength at 90 days.

The reason is that the finer aggregate gradation has a lower content of coarse particles, and the coarse aggregate mixture is suspended and cannot form a dense skeleton. At this time, the strength of HPC mainly depends on the strength of the cement paste matrix; the coarser aggregate gradation in the mixture has a higher content of coarse particles and a lower specific surface area, and the large aggregate that surrounds the transition zone has a lower bond strength during HPC loading because the smaller specific surface area of large particles makes large particles have less connection strength with the hydration product than small particles. Therefore, the appropriate aggregate gradation and particle volume ratio increases can redistribute the internal stress in the sample during HPC loading. The aggregate inhibits the shrinkage of the deformable cement slurry matrix under a compressive load, which shows a higher capacity.

## 5. Results and Discussion of the Concrete Microstructure

### 5.1. Microstructure of the HPC

From the above discussion, the gradation of the aggregate and type of mixtures have a major influence on the mechanical properties of HPC. To reveal the mechanism of manufactured sand HPC, a series of microscopic tests were performed on the matrix of the HPC hydration product over 90 days.

#### 5.1.1. MIP Test

Ten groups of concrete hydration products were tested by mercury injection porosimetry (MIP). The pore distribution curves are presented in Figure 9a–c, and the porosity distribution features are shown in Table 3. Figure 9 shows a significant decrease in porosity and average pore diameter in the admixture HPC compared to the reference concrete pore structure. Among them, the total porosity (pore diameter 5 nm–1000  $\mu\text{m}$ ) and average pore diameter (4 V/A) of the admixture HPC (MS-M-3) were 10.6% and 24.3 nm, respectively, which are far lower than those of RC, whose corresponding values were 20.5% and 69.4 nm. Consequently, the MIP tests clearly show that the HPC consisting of manufactured sand had a high moisture content.

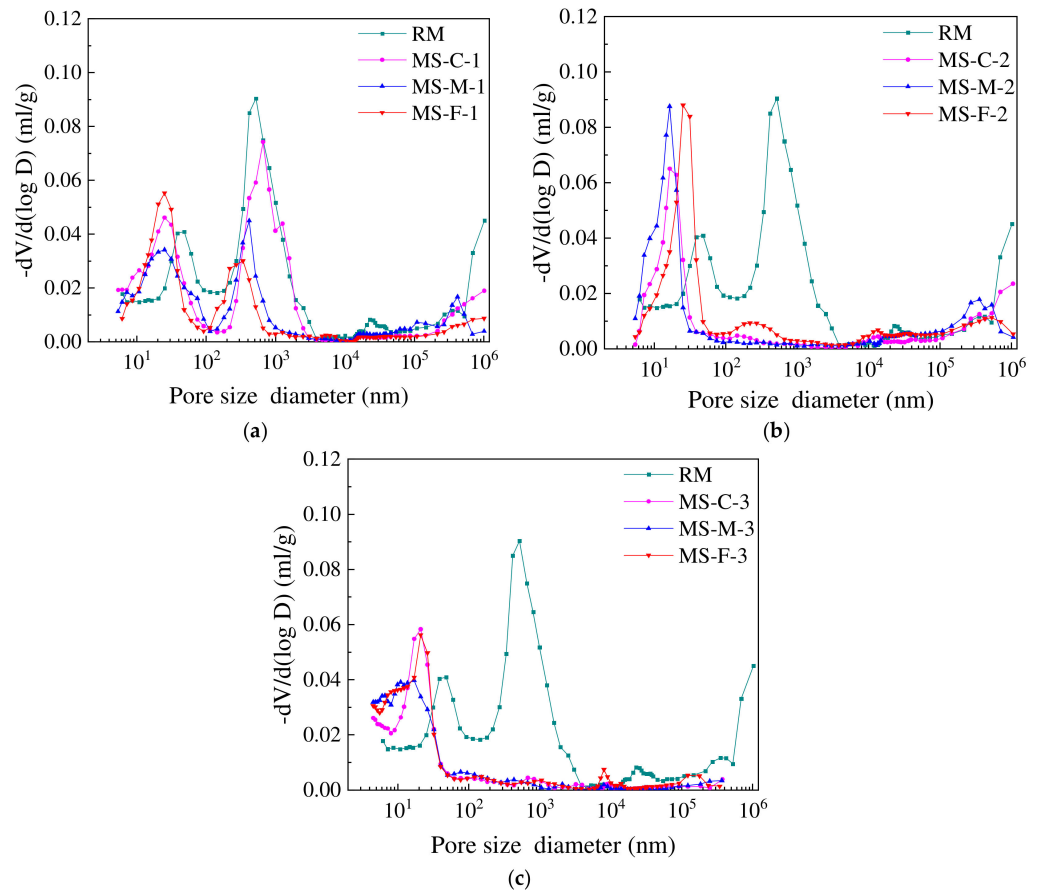


**Figure 9.** Differential pore size of the HPC distribution curve. (a) Single FA; (b) Double mixing FA and SF; (c) Three admixtures of FA, SF, and RM.

**Table 3.** Concrete porosity distribution, average pore diameter, and total porosity.

Mix No.	Pore Size Distribution (%)				Average Pore Size (4 V/A) (nm)	Porosity (%)
	$d \leq 20$ nm	$20 \text{ nm} \leq d \leq 50$ nm	$50 \text{ nm} \leq d \leq 200$ nm	$d > 200$ nm		
RC	8.3	13.6	10.4	67.6	69.4	20.5
MS-C-1	29.2	31.5	6.2	33.0	25.7	12.4
MS-M-1	21.8	22.2	14.1	41.8	34.5	12.5
MS-F-1	29.1	35.4	4.4	31.1	26.9	11.4
MS-C-2	19.9	12.4	21.4	46.3	25.1	10.0
MS-M-2	14.4	21.1	27.6	36.8	23.2	12.7
MS-F-2	35.6	32.1	3.5	29.2	37.7	13.8
MS-C-3	50.5	6.9	4.6	37.8	21.5	11.8
MS-M-3	50.1	3.6	2.2	44.2	24.3	10.6
MS-F-3	27.1	24.7	5.4	42.7	42.2	13.9

According to the classification method of academician Wu Zhongwei of the Chinese Academy of Engineering [31], a pore diameter less than 20 nm is a harmless grade pore, a pore diameter of 20–50 nm is a less harmful grade pore, a pore diameter of 50–200 nm is a harmful grade pore, and a pore diameter above 200 nm is a multiple harmful grade pore. As seen from Table 3, the proportion of harmless grade pores of triple mixture concrete with fly ash, silica fume, and red mud powder was up to nearly 50%; among them, the less harmful grade pores and harmful grade pores of middle mesh size concrete (MS-M-3) were the lowest (3.6% and 2.2%, respectively). The harmless grade pore decreased by 6 times, and the less harmful grade pore and harmful grade pore decreased by 3.8 times and 4.7 times, respectively, compared to the reference mixture group concrete.

#### 5.1.2. SEM Test

The surface morphology of reference concrete (RC), single mixture FA (MS-M-1), double mixtures FA and SF (MS-M-2) and the hydration products of triple mixtures FA, SF, and RM (MS-M-3) were studied by SEM tests. The surface morphology pictures are shown in Figure 10a–d, respectively. In Figure 10a, the lower left side shows aggregates, and the upper right side presents hydrate products, such as hydrated calcium–silicate gel, flake calcium hydroxide and amorphous aluminum silicate. A gap approximately 1  $\mu\text{m}$  wide between the hydration matrix and the aggregates can be clearly observed, and the interface is weakly bonded. The components of the moisture product in Figure 10a,b look more similar. Figure 10b shows that the upper left side of the ITZ between coarse aggregate and HPC paste is very dense and strong. However, non-hydrated fly ash particles with diameters of approximately 2–5  $\mu\text{m}$  can be clearly observed in the concrete containing FA. The main component of hydrate in Figure 10c is a hydrated calcium–silicate gel. The bond of aggregate and ITZ paste have been completely integrated with the hydrate, and the relatively dense surface structure is clearly observed. The highly developed hydrate product paste intertwined with hydrated calcium–silicate gel, calcium hydroxide and calcium, iron element, etc., pastes to form a stereoscopic honeycomb structure, as shown in Figure 10d.

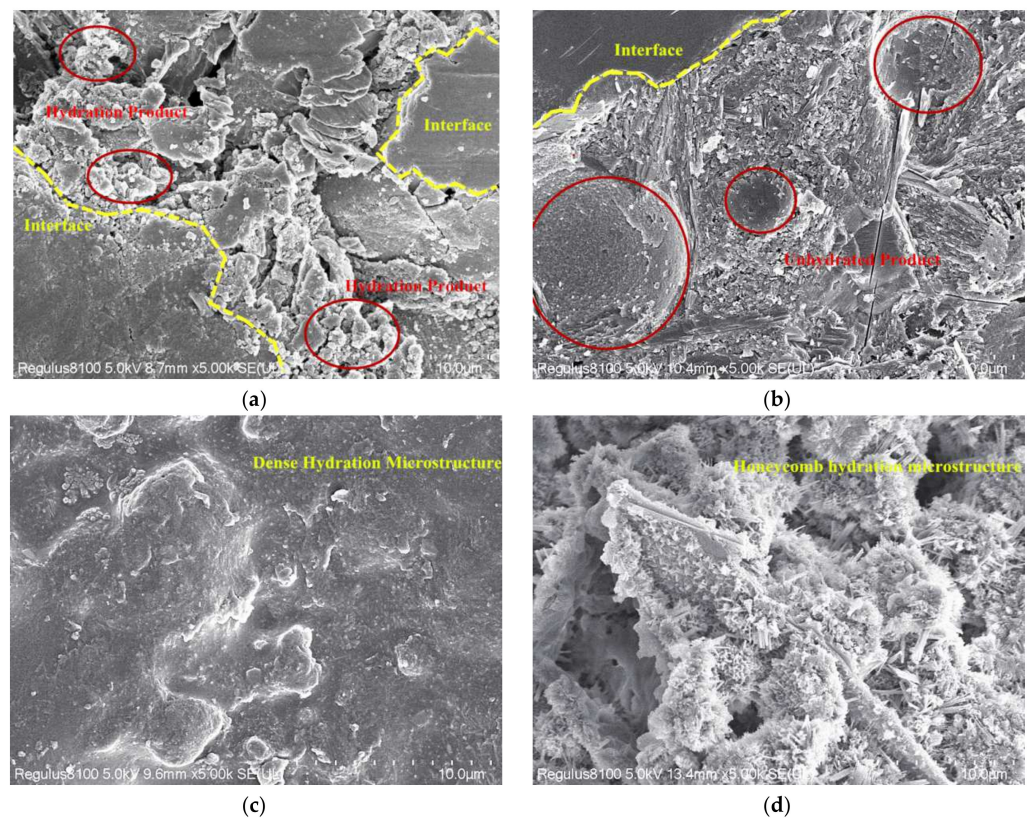


**Figure 10.** SEM photos of the hydration products. (a) RC group; (b) Single FA; (c) Double mixing FA and SF; (d) Three admixtures of FA, SF, and RM.

### 5.1.3. EDS Tests

The EDS test was conducted on the specimens of reference mixture concrete, single mixture with FA, double mixtures with FA and SF, and the hydration products of triple mixtures with FA, SF, and RM, which are shown in Figure 11a–d. More calcium silicate and calcium sulfoaluminate components were found in the reference mixture specimen; however, obvious changes were observed in the EDS spectrum of the HPC admixture. The strength of the “Ca peak” in calcium silicate was greatly enhanced. This result indicates a pozzolane reaction between admixture (FA, SF, and RM) and cement clinker. A great amount of calcium hydrate silicate gel is produced. This reaction obviously enhances the matrix and ITZ of HPC.

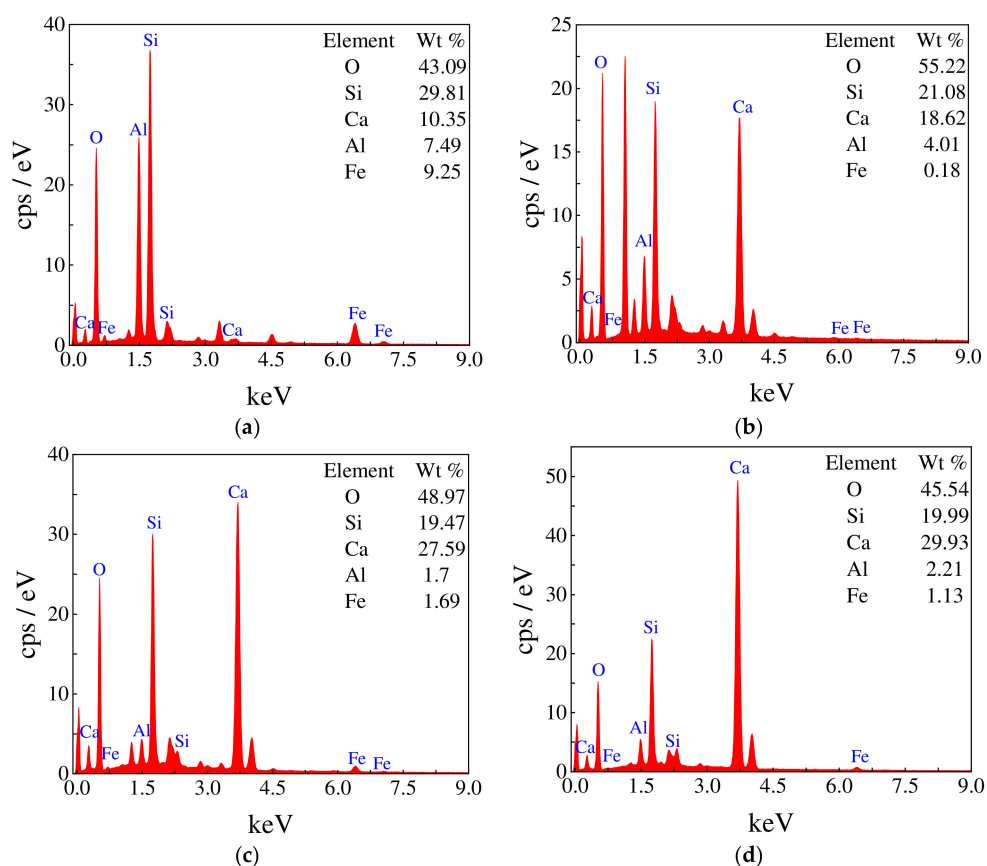


**Figure 11.** EDS of the reference group concrete and admixture concrete. (a) RC group; (b) Single FA; (c) Double mixing FA and SF; (d) Three admixtures of FA, SF, and RM.

### 5.2. Mechanism Discussion

Based on the microscopic tests, the strength enhancement mechanism for HPC containing manufactured sand is discussed. Concrete is an anisotropic material, and its performance mainly depends on the composition of the cementitious material hydration product, aggregate gradation, and mineral character. The ITZ of common normal concrete is a structural layer up to 50  $\mu\text{m}$  wide. The reference mixture mercury injection porosimeter (MIP) measurement in Figure 9 shows that the pore diameter is 104~105 nm [32]. Figure 10 shows a higher level of calcium hydroxide (CH) and ettringite ( $3\text{CaO}\cdot\text{Al}_2\text{O}_3\cdot 3\text{CaSO}_4\cdot < 30\sim 32 > \text{H}_2\text{O}$ ) in the reference mixture with respect to the hydrate slurry of the admixture. Thus, interfaces are the weakest link in concrete and play a very important role in the failure process.

However, the HPC failure process is very different from that of the reference mixture. The mixture has a much more significant influence on the mechanical properties of HPC than the reference mixture. This result can be attributed to the following reasons. First, similar to the EDS test results in Figure 11 and Table 4, the ITZ of the HPC admixture is very dense, and the porosity is low with increasing admixture type. Because a lignin sulfonate high-efficiency water reducer is used, the HPC can be made with a very low water-binder ratio, an optimized mixture process, good cohesiveness, and high mobility. In addition, the particle sizes of FA, SF, and RM are small, which present the microaggregate effect in the matrix of concrete cement paste. Therefore, the gaps of manufactured sand aggregates suspended in the cement slurry matrix are highly compacted by the mineral admixture, and the synergistic effect leads to the very low porosity of the matrix of concrete cement paste, which results in the high strength of the C50 HPC.

**Table 4.** Main elements of the hydration product contents.

Total Number Spectrum of Distribution Element	Element Content (%)			
	(a)	(b)	(c)	(d)
O	43.09	55.22	48.97	45.54
Si	29.81	21.08	19.47	19.99
Ca	10.35	18.62	27.59	29.93
Al	7.49	4.01	1.7	2.21
Fe	9.25	0.18	1.69	1.13
Total:	99.99	100.00	99.42	98.8

Second, as discussed above, the failure of normal concrete tends to begin and develop from the ITZ. However, the ITZ of the admixture HPC is extremely enhanced with the types of admixture, as shown in the SEM image in Figure 10a–d. The ITZ enhancement can be attributed to the pozzolanic reaction of mineral admixtures, including FA, SF, and RM. The main useful effect of the mixture in the HPC consists of a “supercomposite effect”, which comprises a microaggregate filling effect and a pozzolanic reaction. FA, SF, and RM mainly consist of  $Al_2O_3$ ,  $Fe_2O_3$ , and  $SiO_2$ , which can be activated with alkaline substances, such as calcium hydroxide, to form compounds with cementitious material hydration products under water conditions. The two hydrated products of cement hydration are calcium–silicate–hydrate (C-S-H) and calcium hydroxide (CH). C-S-H is the main contributor to the strength of the concrete. The mineral admixture of FA, SF, and RM contains amorphous silica reactive  $SiO_2$ , which reacts with CH to form additional C-S-H and improves the strength. The EDS test results in Figure 11 demonstrate that the C50 HPC mixture has much more C-S-H than the reference group pure cement concrete. As a result, the ITZ in the HPC has been greatly improved. The aggregate and matrix of cement paste work together to form a dense stereoscopic honeycomb texture, and their potential strength can be fully used.

## 6. Conclusions

In this study, 50-MPa HPC was successfully prepared with high fluidity and compressive strength by utilizing composite mineral admixtures consisting of FA, SF, and RM to replace 15% of silicate cement. Continuous gradation manufactured sand with a maximal diameter of 37.5 mm was used to totally replace the concrete coarse aggregate and river aggregate (fine aggregate), which applied homemade efficient lignin sulfonate as a thickening agent and water reducer.

- (1) C50 HPC with coarse aggregate has many advantages over conventional concrete; for example, all aggregates are locally sourced and belong to waste utilization, low production and transportation costs, and preservation of natural resources.
- (2) The larger specific surface area of the superfine mixing powder and high water demand affect the workability of the fresh C50 HPC. In addition, aggregate particles that are too coarse or too fine may decrease the HPC workability.
- (3) The type of aggregate significantly impacts the compressive strength of C50 HPC. The medium gradation aggregate and mixture containing FA, SF, and RM help improve the HPC compressive strength.
- (4) The excellent and low porosity performance of manufactured sand C50 HPC is mainly attributed to the rational design of the mixture with cementitious systems containing silicate cement clinker, FA, SF, and RM. The superfilling effect, pozzolanic reaction, and microaggregate effect of the composite admixtures result in highly developed hydration products, produce a synergistic effect, and form a dense stereoscopic honeycomb structure with low porosity and strong ITZ bonding between matrix and aggregate.
- (5) Compound admixture of C50 HPC with FA, SF, and RM had a good fluidity and the highest compressive strength. It can be seen from the microscopic analysis that the concrete with MS-M grading was rich in hydration products, forming a honeycomb

network structure, and the pore structure was mainly distributed in the range of less harmful holes. At this time, the comprehensive performance of concrete was the best.

**Author Contributions:** Conceptualization, Y.W. and Y.H.; methodology, Y.W. and Y.H.; validation, Y.W. and Y.H.; formal analysis, L.Z. and Y.H.; investigation, Y.H., L.Z. and W.Z.; data curation, L.Z. and Y.H.; writing—original draft preparation, Y.H.; writing—review and editing, Y.H. and S.C.; project administration, Y.W. and W.Z.; funding acquisition, Y.W. and Y.H. All authors have read and agreed to the published version of the manuscript.

**Funding:** This research was financially supported by the National Natural Science Foundation of China (No. 51778300) and the Priority Academic Program Development Jiangsu Higher Education Institutions (PAPD).

**Institutional Review Board Statement:** Not applicable.

**Informed Consent Statement:** Not applicable.

**Data Availability Statement:** The data presented in this study are available on request from the corresponding author.

**Acknowledgments:** We thank Su Fan and Yang Jing of the Advanced Analysis and Testing Center of Nanjing Forestry University for the help with the EDS and SEM tests.

**Conflicts of Interest:** The authors declare no conflict of interest.

## References

1. Zhang, P.; Hu, J.; Zhao, K.X.; Chen, H.; Zhao, S.D.; Li, W.W. Dynamics and decoupling analysis of carbon emissions from construction industry in China. *Buildings* **2022**, *12*, 257. [[CrossRef](#)]
2. Makul, N.; Fediuk, R.; Amran, M.; Zeyad, A.M.; de Azevedo, A.R.G.; Klyuev, S.; Vatin, N.; Karelina, M. Capacity to develop recycled aggregate concrete in South East Asia. *Buildings* **2021**, *11*, 234. [[CrossRef](#)]
3. Gradinaru, C.M.; Barbuta, M.; Ciocan, V.; Serbanoiu, A.A. (Eds.) A study on the effects of the cement and mineral aggregates replacement with waste materials. In Proceedings of the 3rd China-Romania Science and Technology Seminar (CRSTS), Brasov, Romania, 24–27 April 2018; Iop Publishing Ltd.: Bristol, UK, 2018.
4. Silva, I.; Castro-Gomes, J.; Albuquerque, A. Mineral waste geopolymeric artificial aggregates as alternative materials for wastewater-treatment processes: Study of structural stability and pH variation in water. *J. Mater. Civ. Eng.* **2012**, *24*, 623–628. [[CrossRef](#)]
5. Li, L.J.; Mai, G.H.; He, S.H.; Xiong, Z.; Wei, W.; Luo, H.W.; Liu, F. Experimental study on bond behaviour between recycled aggregate concrete and basalt fibre-reinforced polymer bars under different strain rates. *Constr. Build. Mater.* **2021**, *290*, 123218. [[CrossRef](#)]
6. Chu, S.H.; Poon, C.S.; Lam, C.S.; Li, L. Effect of natural and recycled aggregate packing on properties of concrete blocks. *Constr. Build. Mater.* **2021**, *278*, 122247. [[CrossRef](#)]
7. Arulmoly, B.; Konthesingha, C.; Nanayakkara, A. Performance evaluation of cement mortar produced with manufactured sand and offshore sand as alternatives for river sand. *Constr. Build. Mater.* **2021**, *297*, 123784. [[CrossRef](#)]
8. Guan, M.S.; Liu, W.T.; Lai, M.H.; Du, H.B.; Cui, J.; Gan, Y.Y. Seismic behaviour of innovative composite walls with high-strength manufactured sand concrete. *Eng. Struct.* **2019**, *195*, 182–199. [[CrossRef](#)]
9. Shen, W.G.; Liu, Y.; Cao, L.H.; Huo, X.J.; Yang, Z.G.; Zhou, C.C.; He, P.; Lu, Z. Mixing design and microstructure of ultra high strength concrete with manufactured sand. *Constr. Build. Mater.* **2017**, *143*, 312–321. [[CrossRef](#)]
10. Vijaya, B.; Selvan, S.S.; Vasanthi, P. (Eds.) Experimental investigation on the behaviour of reinforced concrete column containing manufactured sand under axial compression. In Proceedings of the 3rd International Conference on Advanced Materials and Modern Manufacturing (ICAMMM), Tamil Nadu, India, 3–4 April 2020.
11. Zhang, H.; Bai, L.Y.; Qi, Y.Z.; Hong, H.; Neupane, A.; Pan, Q. Impact of splitting tensile properties and dynamic constitutive model of fly ash concrete. *J. Mater. Civ. Eng.* **2020**, *32*, 04020225. [[CrossRef](#)]
12. Guo, Y.Y.; Zhang, Y.X.; Soe, K.; Hutchison, W.D.; Timmers, H.; Poblete, M.R. Effect of fly ash on mechanical properties of magnesium oxychloride cement under water attack. *Struct. Concr.* **2020**, *21*, 1181–1199. [[CrossRef](#)]
13. Sothornchaiwit, K.; Dokduea, W.; Tangchirapat, W.; Keawsawasvong, S.; Thongchom, C.; Jaturapitakkul, C. Influences of silica fume on compressive strength and chemical resistances of high calcium fly ash-based alkali-activated mortar. *Sustainability* **2022**, *14*, 2652. [[CrossRef](#)]
14. Kapeluszna, E.; Kotwica, L.; Nocun-Wczelik, W. Comparison of the effect of ground waste expanded perlite and silica fume on the hydration of cements with various tricalcium aluminate content—Comprehensive analysis. *Constr. Build. Mater.* **2021**, *303*, 124434. [[CrossRef](#)]

15. Koksai, F.; Kocabeyoglu, E.T.; Gencil, O.; Benli, A. The effects of high temperature and cooling regimes on the mechanical and durability properties of basalt fiber reinforced mortars with silica fume. *Cem. Concr. Compos.* **2021**, *121*, 104107. [[CrossRef](#)]
16. Nguyen, H.T.; Do, Q.M. Preparation of a novel cement from red mud and limestone. *Int. J. Eng. Res. Afr.* **2022**, *58*, 171–182. [[CrossRef](#)]
17. Richard, P.; Cheyrezy, M. Composition of reactive powder concretes. *Cem. Concr. Res.* **1995**, *25*, 1501–1511. [[CrossRef](#)]
18. Radlinski, M.; Olek, J. Investigation into the synergistic effects in ternary cementitious systems containing portland cement, fly ash and silica fume. *Cem. Concr. Compos.* **2012**, *34*, 451–459. [[CrossRef](#)]
19. He, H.; Wang, Y.L.; Wang, J.J. Effects of aggregate micro fines (AMF), aluminum sulfate and polypropylene fiber (PPF) on properties of machine-made sand concrete. *Appl. Sci.* **2019**, *9*, 2250. [[CrossRef](#)]
20. Shi, J.Y.; Tan, J.X.; Liu, B.J.; Chen, J.Z.; Dai, J.D.; He, Z.H. Experimental study on full-volume slag alkali-activated mortars: Air-cooled blast furnace slag versus machine-made sand as fine aggregates. *J. Hazard. Mater.* **2021**, *403*, 123983. [[CrossRef](#)]
21. Zhang, R.L.; Wang, Q.C.; Ma, L.-N.; Li, X.-D. Compound admixture system effect on high performance concrete shrinkage performance. *Bull. Chin. Ceram. Soc.* **2013**, *32*, 2194–2199.
22. Liu, Y.; Li, H.; Wang, K.; Wu, H.F.; Cui, B.Q. Effects of accelerator-water reducer admixture on performance of cemented paste backfill. *Constr. Build. Mater.* **2020**, *242*, 118187. [[CrossRef](#)]
23. Huang, C.X.; Ma, J.M.; Zhang, W.Y.; Huang, G.; Yong, Q. Preparation of lignosulfonates from biorefinery lignins by sulfomethylation and their application as a water reducer for concrete. *Polymers* **2018**, *10*, 841. [[CrossRef](#)]
24. BS. *Aggregates for Concrete*; EN: London, UK, 2020; p. 12620.
25. Wang, Y.W.; Wang, L.; Hu, Z.; Li, Y.L.; Sun, Q.; Liu, A.X.; Yang, L.; Gong, J.; Guo, X. The thermodynamic and kinetic effects of sodium lignin sulfonate on ethylene hydrate formation. *Energies* **2021**, *14*, 3291. [[CrossRef](#)]
26. Sun, J.W.; Feng, J.J.; Chen, Z.H. Effect of ferronickel slag as fine aggregate on properties of concrete. *Constr. Build. Mater.* **2019**, *206*, 201–209. [[CrossRef](#)]
27. BS. *Testing Fresh Concrete—Part 2: Slump Test*; EN: London, UK, 1999; p. 12350-2.
28. BS. *Testing Hardened Concrete—Part 3: Compressive Strength of Test Specimens*; EN: London, UK, 2001; p. 12390-3.
29. Ma, H.; Sun, Z.J.; Ma, G.G. Research on compressive strength of manufactured sand concrete based on response surface methodology (RSM). *Appl. Sci.* **2022**, *12*, 3506. [[CrossRef](#)]
30. Ding, X.X.; Li, C.Y.; Xu, Y.Y.; Li, F.L.; Zhao, S.B. Experimental study on long-term compressive strength of concrete with manufactured sand. *Constr. Build. Mater.* **2016**, *108*, 67–73. [[CrossRef](#)]
31. Wu, Z.W. High performance concrete-green concrete. *China Concr. Cem. Prod.* **2000**, *1*, 3–6.
32. Lv, Y.J.; Zhang, W.H.; Wu, F.; Wu, P.P.; Zeng, W.Z.; Yang, F.H. Static mechanical properties and mechanism of C200 ultra-high performance concrete (UHPC) containing coarse aggregates. *Sci. Eng. Compos. Mater.* **2020**, *27*, 186–195.